Secrecy Performance of Correlated α-μ Fading Channels

Aashish Mathur, *Member, IEEE,* Yun Ai, *Member, IEEE*, Michael Cheffena, and Georges Kaddoum, *Member IEEE*

***Abstract*—This paper investigates the secrecy performance of the classical Wyner's wiretap model, where the main channel and eavesdropper channel experience correlated α-μ fading. Novel and exact expressions for the average secrecy capacity and secrecy outage probability are derived for the considered realistic scenario. The effect of correlation has been studied on the secrecy performance. Useful insights into the system performance are obtained through the asymptotic analysis.**

***Index Terms*—Fading correlation, α-μ fading, physical layer security, average secrecy capacity, secrecy outage probability.**

I. Introduction

PHYSICAL LAYER SECURITY (PLS) has been widely considered as a complementary technique to the conventional upper layer cryptography to enhance the communication secrecy against eavesdropping in the fifth generation (5G) mobile networks [1]. In real radio environments, correlations between channels are frequently observed due to antenna deployments, proximity of the legitimate receiver and eavesdropper, and scatterers around them [2], [3]. For example, antenna deployments at high altitude in rural or suburban area generate dominant line-of-sight paths, which results in high correlation between the received signals at two receivers. Intuitively, correlated channel conditions will lead to some level of degradation of secrecy performance, therefore it is also possible that the eavesdropper intentionally places itself close to the legitimate receiver (especially when the eavesdropper has no information on the whereabouts of the transmitter) to induce the correlation of the corresponding channels. Therefore, it is important to quantify rigorously the effects of correlation in real-life practical scenarios. Due to the frequent occurrences of correlated fading scenarios in real-life scenarios, the investigations on secrecy performance over correlated fading channels has recently attracted attention of the researchers [3], [4].

The recently proposed α-μ fading model is a general and flexible instrument for channel characterization and performance evaluation of communication systems. The α-μ model encompasses some important distributions such as exponential, Nakagami-m, Gamma, Weibull, Rayleigh, log-normal and Generalized-K (used in free space optical communication) fading, [5]–[7]; and the characterization of PLS over α-μ wiretap fading channels is decisively important. Revisiting all existing work on secrecy analysis of α-μ fading channels [6], [7], the correlation between the α μ fading links has never been considered to the best of the authors' knowledge. Motivated by the latest advances in PLS analysis on α μ fading channels [6], [7] and the importance of conducting secrecy analysis under realistic correlated fading scenarios, we study the secrecy performance of the Wyner's model over correlated α-μ fading channels in this paper. The main contributions of this letter are summarized as follows:

1) A novel and exact expression for the average secrecy capacity (ASC) is derived in terms of the extended generalized bivariate Fox H-function (EGBFHF) for the classical Wyner's model under the realistic correlated α-μ fading scenario contrary to [7], where the effect of correlation was ignored.
2) Exact expression for the secure outage probability (SOP) is obtained taking into account the correlation between the main wiretap channels contrary to [6], where only bounds on SOP were provided and correlation was ignored.
3) We obtain useful insights into the impact of correlation on the secrecy performance through asymptotic analysis of the ASC and SOP.
4) The asymptotic SOP results are instrumental in investigating the impact of physical channel phenomena such as channel nonlinearity and multipath clustering on secrecy diversity.
5) The effect of correlation dependent power penalty is also studied in this letter.

Notations: $[x]^+ = \max(x, 0)$. $\mathrm{E}(\cdot)$ denotes the expectation operator, $L_m^n(\cdot)$ is the Laguerre polynomial [8, Eq. (8.970.1)], $\Gamma(\cdot)$ is the Gamma function [8, Eq. (8.310)], $\Upsilon(\cdot,\cdot)$ is the lower incomplete Gamma function [8, Eq. (8.350.1)], $\Delta(k,a) = \frac{a}{k}, \frac{a+1}{k}, ..., \frac{a+k-1}{k}$, $H_{p,q:t,u:w,x}^{m,n;r,s;v,u}(\cdot)$ denotes the EGBFHF [7], $G_{p,q}^{m,n}\left(x \begin{smallmatrix} a_1,...,a_p \\ b_1,...,b_q \end{smallmatrix}\right)$ is the Meijer G-function [8, Eq. (9.343)], and $(\cdot)_k$ is the Pochhammer's symbol [9, Eq. (6.1.22)].

II. Channel and System Models

Considering the classic Wyner's wiretap model [10], the legitimate source *S* transmits confidential information signal to the legitimate destination node *D* over the main channel. The eavesdropper *E* attempts to intercept the information by decoding its received signal from the eavesdropper channel. It is assumed that the main and eavesdropper channels experience correlated α-μ fading due to antenna deployments, proximity or similarity of scatterers around them [2], [3]. The channel coefficients are assumed to remain constant during a block period.

The received signal at node *X*, $X \in \{D, E\}$, is expressed as

$$y_X = h_X x + w, \tag{1}$$

where x is the transmitted signal with energy E_s, h_X denotes the channel between node *S* and *X*, w represents the additive white Gaussian noise (AWGN) with power spectral density N_0, which, without loss of generality, is assumed to be the same for both channel links.

A. Mathur is with the Department of Electrical Engineering, Indian Institute of Technology Jodhpur, Jodhpur, 342037, India (e-mail: aashish-mathur@iitj.ac.in).

Y. Ai and M. Cheffena are with the Faculty of Engineering, Norwegian University of Science and Technology, 2815 Gjovik, Norway (e-mails: yun.ai@ntnu.no, michael.cheffena@ntnu.no).

G. Kaddoum is with the Department of Electrical Engineering, Ecole de technologie superieure, Montreal QC H3C 1K3, Canada. (e-mail: georges.kaddoum@etsmtl.ca).

$$C_1 = \frac{1}{\Gamma(\mu_D)\Gamma(\mu_E)} \sum_{k=0}^{\infty} \frac{(1/2)_k k! \rho^{2k}}{(\mu_D)_k (\mu_E)_k} \sum_{l=0}^{k} \frac{(-1)^l}{l!} \binom{k+\mu_E-1}{k-l} \sum_{m=0}^{k} \frac{(-1)^m}{m!} \binom{k+\mu_D-1}{k-m} \times H_{1,0:2,2:1,2}^{0,1:1,2:1,1} \left(\begin{matrix} (1-(\mu_D+m)); \frac{2}{\alpha_D}, \frac{\alpha_E}{\alpha_D} \\ - \end{matrix} \middle| \begin{matrix} (1,1),(1,1) \\ (1,1),(0,1) \end{matrix} \middle| \begin{matrix} (1,1) \\ (\mu_E+l,1),(0,1) \end{matrix} \middle| \begin{matrix} \frac{\bar{\gamma}_D}{(\psi'_D)^{\frac{2}{\alpha_D}}}, \frac{{\psi'}_E}{(\psi'_D)^{\frac{\alpha_E}{\alpha_D}} \left(\frac{\bar{\gamma}_E}{\bar{\gamma}_D}\right)^{\frac{\alpha_E}{2}}} \end{matrix} \right). \quad (7)$$

$$C_2 = \frac{1}{\Gamma(\mu_D)\Gamma(\mu_E)} \sum_{k=0}^{\infty} \frac{(1/2)_k k! \rho^{2k}}{(\mu_D)_k (\mu_E)_k} \sum_{l'=0}^{k} \frac{(-1)^{l'}}{l'!} \binom{k+\mu_D-1}{k-l'} \sum_{m'=0}^{k} \frac{(-1)^{m'}}{m'!} \binom{k+\mu_E-1}{k-m'} \times H_{1,0:2,2:1,2}^{0,1:1,2:2,0} \left(\begin{matrix} (1-(\mu_E+m')); \frac{2}{\alpha_E}, \frac{\alpha_D}{\alpha_E} \\ - \end{matrix} \middle| \begin{matrix} (1,1),(1,1) \\ (1,1),(0,1) \end{matrix} \middle| \begin{matrix} (1,1) \\ (0,1),(\mu_D+l',1) \end{matrix} \middle| \begin{matrix} \frac{\bar{\gamma}_E}{(\psi'_E)^{\frac{2}{\alpha_E}}}, \frac{{\psi'}_D}{(\psi'_E)^{\frac{\alpha_D}{\alpha_E}} \left(\frac{\bar{\gamma}_D}{\bar{\gamma}_E}\right)^{\frac{\alpha_D}{2}}} \end{matrix} \right). \quad (8)$$

From (1), the instantaneous signal-to-noise ratio (SNR), γ_X, received at node *X*, $X \in \{D, E\}$, can be expressed as

$$\gamma_X = \frac{{h_X}^2 E_s}{N_0}. \quad (2)$$

The joint α-μ probability density function (PDF) of the correlated SNR can be written using [11, Eq. (28)] with $L = 2$ and $C_{12} = \rho^2$ [11, Eq. (6) and Eq. (10)]:

$$f_{\gamma_D,\gamma_E}(\gamma_D,\gamma_E) = \frac{\alpha_D \alpha_E {\psi'_D}^{\mu_D} {\psi'_E}^{\mu_E} \gamma_D^{\frac{\alpha_D \mu_D}{2} - 1} \gamma_E^{\frac{\alpha_E \mu_E}{2} - 1}}{4\Gamma(\mu_D)\Gamma(\mu_E) \bar{\gamma}_D^{\frac{\alpha_D \mu_D}{2}} \bar{\gamma}_E^{\frac{\alpha_E \mu_E}{2}}} \times \exp\left(-\frac{\psi'_D \gamma_D^{\frac{\alpha_D}{2}}}{\bar{\gamma}_D^{\frac{\alpha_D}{2}}}\right) \exp\left(-\frac{\psi'_E \gamma_E^{\frac{\alpha_E}{2}}}{\bar{\gamma}_E^{\frac{\alpha_E}{2}}}\right) \sum_{k=0}^{\infty} \frac{(1/2)_k \rho^{2k} k!}{(\mu_D)_k (\mu_E)_k} \times L_k^{\mu_D - 1}\left(\frac{\psi'_D \gamma_D^{\frac{\alpha_D}{2}}}{\bar{\gamma}_D^{\frac{\alpha_D}{2}}}\right) L_k^{\mu_E - 1}\left(\frac{\psi'_E \gamma_E^{\frac{\alpha_E}{2}}}{\bar{\gamma}_E^{\frac{\alpha_E}{2}}}\right). \quad (3)$$

In (3), $\rho \in (0, 1]$ is the correlation coefficient between the SNRs γ_D and γ_E; α_X is the nonlinearity parameter due to the propagation of clusters of multipath waves in a nonhomogeneous environment and μ_X denotes the number of multipath clusters [5]. The parameter $\gamma_X = \frac{\mathrm{E}({h_X}^2) \cdot E_s}{N_0}$ denotes the average SNR of the corresponding link and $\psi'_X = \left(\frac{\Gamma(\mu_X + 2/\alpha_X)}{\Gamma(\mu_X)}\right)^{\frac{\alpha_X}{2}}$.

Remark 1: When $\rho = 0$, the PDF in (3) reduces to the product of marginal PDFs of D and E using [11, Eq. (33)] as $g(\beta_1, \beta_2) = 1$ [11, Eq. (6)] and $C_{ij} = 0$ [11, Eq. (10)]. The ASC and SOP results of [6], [7] will apply.

III. Average Secrecy Capacity Analysis

Under active eavesdropping, the node *S* has full channel state information (CSI) of both the main and eavesdropper channels, from which *S* can adapt the achievable secrecy rate accordingly [12]. In this case, the instantaneous secrecy capacity of the considered system is defined as $C_s(\gamma_D, \gamma_E) = [\ln(1+\gamma_D) - \ln(1+\gamma_E), 0]^+$ [13]. The ASC, $\overline{C}_s$, over the correlated α-μ fading channels can be evaluated as [4]

$$\begin{aligned} \overline{C}_s &= \int_0^{\infty}\int_0^{\infty} C_s(\gamma_D,\gamma_E) \cdot f_{\gamma_D,\gamma_E}(\gamma_D,\gamma_E)\, d\gamma_D d\gamma_E \\ &= \int_0^{\infty} \ln(1+\gamma_D) \int_0^{\gamma_D} f_{\gamma_D,\gamma_E}(\gamma_D,\gamma_E) d\gamma_E d\gamma_D \\ &\quad - \int_0^{\infty} \ln(1+\gamma_E) \int_{\gamma_E}^{\infty} f_{\gamma_D,\gamma_E}(\gamma_D,\gamma_E) d\gamma_D d\gamma_E \\ &= C_1 - C_2. \end{aligned} \quad (4)$$

On substituting (3) in the expression for C_1, utilizing the series expansion for the Laguerre polynomial [8, Eq. (8.970.1)], and then applying the transformation $\gamma_E^{\alpha_E/2} = t$, C_1 can be re-written using [8, Eq. (3.381.1)] as

$$C_1 = \frac{\alpha_D {\psi'_D}^{\mu_D}}{2\Gamma(\mu_D)\Gamma(\mu_E)\bar{\gamma}_D^{\frac{\alpha_D \mu_D}{2}}} \sum_{k=0}^{\infty} \frac{(1/2)_k \rho^{2k} k!}{(\mu_D)_k (\mu_E)_k} \sum_{l=0}^{k} \frac{(-1)^l}{l!} \times \binom{k+\mu_E-1}{k-l} \int_0^{\infty} \ln(1+\gamma_D) \gamma_D^{\frac{\alpha_D \mu_D}{2} - 1} \exp\left(-\frac{\psi'_D \gamma_D^{\frac{\alpha_D}{2}}}{\bar{\gamma}_D^{\frac{\alpha_D}{2}}}\right) \times L_k^{\mu_D - 1}\left(\psi'_D \left(\frac{\gamma_D}{\bar{\gamma}_D}\right)^{\frac{\alpha_D}{2}}\right) \Upsilon\left(\mu_E + l, \psi'_E \left(\frac{\gamma_D}{\bar{\gamma}_E}\right)^{\frac{\alpha_E}{2}}\right) d\gamma_D. \quad (5)$$

Now, utilizing [8, Eq. (8.970.1)] and the Meijer G representation of $\ln(\cdot)$, $\exp(\cdot)$, and $\Upsilon(\cdot,\cdot)$ from [14, Eqs. (8.4.6.4), (8.4.3.1), and (8.4.16.1)], respectively, the integral in (5) is converted to the following form using [15, Eq. (6.2.8)]:

$$C_1 = \frac{\alpha_D {\psi'_D}^{\mu_D}}{2\Gamma(\mu_D)\Gamma(\mu_E)\bar{\gamma}_D^{\frac{\alpha_D \mu_D}{2}}} \sum_{k=0}^{\infty} \frac{(1/2)_k \rho^{2k} k!}{(\mu_D)_k (\mu_E)_k} \sum_{l=0}^{k} \frac{(-1)^l}{l!} \times \binom{k+\mu_E-1}{k-l} \sum_{m=0}^{k} \frac{(-1)^m {\psi'_D}^m}{m! \bar{\gamma}_D^{\frac{\alpha_D m}{2}}} \binom{k+\mu_D-1}{k-m} \times \int_0^{\infty} \gamma_D^{\frac{\alpha_D(\mu_D+m)}{2} - 1} H_{1,2}^{1,1}\left(\frac{\psi'_E \gamma_D^{\frac{\alpha_E}{2}}}{\bar{\gamma}_E^{\frac{\alpha_E}{2}}} \middle| \begin{matrix} (1,1) \\ (\mu_E+l,1),(0,1) \end{matrix}\right) \times H_{0,1}^{1,0}\left(\frac{\psi'_D \gamma_D^{\frac{\alpha_D}{2}}}{\bar{\gamma}_D^{\frac{\alpha_D}{2}}} \middle| (0,1)\right) H_{2,2}^{1,2}\left(\gamma_D \middle| \begin{matrix} (1,1),(1,1) \\ (1,1),(0,1) \end{matrix}\right) d\gamma_D \quad (6)$$

The integral in (6) can be simplified with the aid of [16, Eq. (2.3)] and is given by (7) at the top of the page. The closed-form expression for C_2 can be obtained in a similar manner and is given by (8) at the top of the page. The ASC can, thus, be evaluated by substituting (7) and (8) in (4). The EGBFHF in (7) and (8) can be efficiently implemented in Mathematica [7] and MATLAB [17].

IV. Secrecy Outage Probability Analysis

The SOP is a useful secrecy performance metric for the passive eavesdropping scenario, where node *S* does not have CSI on the eavesdropper's channel. The SOP is defined as the probability that the instantaneous secrecy capacity is below a predefined secrecy rate R_s [12], i.e.,

$$\begin{aligned} P_o &= \Pr\left[C_s(\gamma_D,\gamma_E) \le R_s\right] = \Pr\left[\gamma_D \le \Theta\gamma_E + \Theta - 1\right] \\ &= \int_0^{\infty} \int_0^{(1+\gamma_E)\Theta - 1} f_{\gamma_D,\gamma_E}(\gamma_D,\gamma_E)\, d\gamma_D d\gamma_E, \end{aligned} \quad (9)$$

$$P_o = \frac{(2\pi)^{0.5-\alpha_E}}{\Gamma(\mu_D)\Gamma(\mu_E)} \sum_{k=0}^{\infty} \frac{(1/2)_k \rho^{2k} k!}{(\mu_D)_k (\mu_E)_k} \sum_{n=0}^{k} \frac{(-1)^n}{n!} \binom{k+\mu_D-1}{k-n} \sum_{p=0}^{k} \frac{(-1)^p 2^{\mu_E+p-0.5}}{p!} \binom{k+\mu_E-1}{k-p} \sum_{r=0}^{\infty} \frac{(-1)^r}{r!} \times \frac{{\psi'_D}^{\mu_D+n+r} \left(\frac{\Theta-1}{\alpha_E \bar{\gamma}_D}\right)^{\frac{\alpha_D(\mu_D+n+r)}{2}}}{(\mu_D+n+r)\Gamma\left(\frac{-\alpha_D(\mu_D+n+r)}{2}\right)} G_{\alpha_E+2,\alpha_E}^{\alpha_E,\alpha_E+2}\left(\frac{4\left(\frac{\Theta\bar{\gamma}_E}{\Theta-1}\right)^{\alpha_E}}{{\psi'_E}^2} \middle| \begin{matrix} \Delta(2, 1-(\mu_E+p)), \Delta(\alpha_E, \frac{\alpha_D(\mu_D+n+r)}{2}+1) \\ \Delta(\alpha_E, 0) \end{matrix} \right). \quad (12)$$

$$P_o = \frac{1}{\Gamma(\mu_D)\Gamma(\mu_E)} \sum_{k=0}^{\infty} \frac{(1/2)_k \rho^{2k} k!}{(\mu_D)_k (\mu_E)_k} \sum_{n=0}^{k} \frac{(-1)^n}{n!} \binom{k+\mu_D-1}{k-n} \sum_{p=0}^{k} \frac{(-1)^p}{p!} \binom{k+\mu_E-1}{k-p} \sum_{r=0}^{\infty} \frac{(-1)^r}{r!} \times \frac{{\psi'_D}^{\mu_D+n+r} \left(\frac{\Theta-1}{\bar{\gamma}_D}\right)^{\frac{\alpha_D(\mu_D+n+r)}{2}}}{(\mu_D+n+r)} \sum_{s=0}^{\frac{\alpha_D(\mu_D+n+r)}{2}} \binom{\frac{\alpha_D(\mu_D+n+r)}{2}}{s} \left(\frac{\Theta\bar{\gamma}_E}{(\Theta-1){\psi'_E}^{\frac{2}{\alpha_E}}}\right)^s \Gamma\left(\mu_E+p+\frac{2s}{\alpha_E}\right). \quad (13)$$

where $\Theta = \exp(R_s) \geq 1$. In order to solve (9), we substitute the joint PDF of γ_D and γ_E from (3) into (9). Further, using [8, Eq. (8.970.1)] and applying the transformation $\gamma_D^{(\alpha_D/2)} = u$, the inner integral in (9) is solved with the aid of [8, Eq. (3.381.1)] to yield

$$P_o = \frac{\alpha_E {\psi'_E}^{\mu_E}}{2\Gamma(\mu_D)\Gamma(\mu_E)\bar{\gamma}_E^{\frac{\alpha_E\mu_E}{2}}} \sum_{k=0}^{\infty} \frac{(1/2)_k \rho^{2k} k!}{(\mu_D)_k (\mu_E)_k} \sum_{n=0}^{k} \frac{(-1)^n}{n!} \times \binom{k+\mu_D-1}{k-n} \int_0^{\infty} \gamma_E^{\frac{\alpha_E\mu_E}{2}-1} \exp\left(\frac{-{\psi'_E}\gamma_E^{\frac{\alpha_E}{2}}}{\bar{\gamma}_E^{\frac{\alpha_E}{2}}}\right) \times L_k^{\mu_E-1}\left(\frac{{\psi'_E}\gamma_E^{\frac{\alpha_E}{2}}}{\bar{\gamma}_E^{\frac{\alpha_E}{2}}}\right) \Upsilon\left(\mu_D+n, \frac{{\psi'_D}(\Theta\gamma_E+\Theta-1)^{\frac{\alpha_D}{2}}}{\bar{\gamma}_D^{\frac{\alpha_D}{2}}}\right) d\gamma_E. \quad (10)$$

Now, using [8, Eq. (8.354.1)] and [8, Eq. (8.970.1)], (10) can be written after some manipulations as

$$P_o = \frac{\alpha_E {\psi'_E}^{\mu_E}}{2\Gamma(\mu_D)\Gamma(\mu_E)\bar{\gamma}_E^{\frac{\alpha_E\mu_E}{2}}} \sum_{k=0}^{\infty} \frac{(1/2)_k \rho^{2k} k!}{(\mu_D)_k (\mu_E)_k} \sum_{n=0}^{k} \frac{(-1)^n}{n!} \times \binom{k+\mu_D-1}{k-n} \sum_{p=0}^{k} \frac{(-1)^p {\psi'_E}^p}{p!\bar{\gamma}_E^{\frac{\alpha_E p}{2}}} \binom{k+\mu_E-1}{k-p} \sum_{r=0}^{\infty} \frac{(-1)^r}{r!} \times \frac{{\psi'_D}^{\mu_D+n+r}(\Theta-1)^{\frac{\alpha_D(\mu_D+n+r)}{2}}}{(\mu_D+n+r)\bar{\gamma}_D^{\frac{\alpha_D(\mu_D+n+r)}{2}}} \int_0^{\infty} \gamma_E^{\frac{\alpha_E(\mu_E+p)}{2}-1} \times \left(1+\frac{\Theta\gamma_E}{\Theta-1}\right)^{\frac{\alpha_D(\mu_D+n+r)}{2}} \exp\left(\frac{-{\psi'_E}\gamma_E^{\frac{\alpha_E}{2}}}{\bar{\gamma}_E^{\frac{\alpha_E}{2}}}\right) d\gamma_E. \quad (11)$$

Depending on the value of $\alpha_D(\mu_D+n+r)/2$, Eq. (11) is solved in the following two ways:

1) $\alpha_D(\mu_D+n+r)/2$ is not an integer: For this case, utilizing [18, Eq. (10)] and substituting $\gamma_E^{\alpha_E/2} = u$, the integral in (11) is converted to a form similar to [14, Eq. (2.24.1.1)]. Hence, the closed-form expression for the SOP is written as (12) at the top of the page.

2) $\alpha_D(\mu_D+n+r)/2$ is an integer: In this case, we expand $(1+\Theta\gamma_E/(\Theta-1))^{\alpha_D(\mu_D+n+r)/2}$ using the Binomial Theorem [9, Eq. (3.1.1)] and then apply the transformation $\gamma_E^{\alpha_E/2} = v$ to get a form similar to [8, Eq. (3.381.4)]. After some simplifications, P_o is given by (13) at the top of the page.

V. Asymptotic Secrecy Performance Analysis

A. Asymptotic ASC Analysis

For the asymptotic ASC analysis, let us assume that $\bar{\gamma}_D = \bar{\gamma}_E = \bar{\gamma} \to \infty$. Using [7, Eq. (6)] and applying the transformation $\gamma_D = x\bar{\gamma}$ and $\gamma_E = y\bar{\gamma}$, the asymptotic ASC is approximated after some simplifications as

$$\overline{C_s} \approx \frac{\alpha_D \alpha_E {\psi'_D}^{\mu_D} {\psi'_E}^{\mu_E}}{4\Gamma(\mu_D)\Gamma(\mu_E)} \sum_{k=0}^{\infty} \frac{(1/2)_k \rho^{2k} k!}{(\mu_D)_k (\mu_E)_k} (I_1 - I_2), \quad (14)$$

where $I_1 = \int_0^{\infty} x^{\frac{\alpha_D\mu_D}{2}-1} e^{-{\psi'_D}x^{\frac{\alpha_D}{2}}} L_k^{\mu_D-1}({\psi'_D}x^{\frac{\alpha_D}{2}}) \ln x \times \int_0^x y^{\frac{\alpha_E\mu_E}{2}-1} e^{-{\psi'_E}y^{\frac{\alpha_E}{2}}} L_k^{\mu_E-1}({\psi'_E}y^{\frac{\alpha_E}{2}}) dy dx$ and $I_2 = \int_0^{\infty} y^{\frac{\alpha_E\mu_E}{2}-1} e^{-{\psi'_E}y^{\frac{\alpha_E}{2}}} L_k^{\mu_E-1}({\psi'_E}y^{\frac{\alpha_E}{2}}) \ln y \int_y^{\infty} x^{\frac{\alpha_D\mu_D}{2}-1} \times e^{-{\psi'_D}x^{\frac{\alpha_D}{2}}} L_k^{\mu_D-1}({\psi'_D}x^{\frac{\alpha_D}{2}}) dx dy$. Employing [8, Eqs. (8.970.1) and (3.381.1)], I_1 can be expressed as

$$I_1 = \frac{4{\psi'_E}^{-\mu_E}}{\alpha_D \alpha_E {\psi'_D}^{\frac{2}{\alpha_D}}} \sum_{i=0}^{k} \frac{(-1)^i}{i!} \binom{k+\mu_E-1}{k-i} \sum_{j=1}^{N} w_j f_1(t_j), \quad (15)$$

where t_j and w_j are the abscissas and weight factors of the Gauss Laguerre integration [9, Eq. (25.4.45], respectively, and $f_1(t) = t^{\mu_D-1} \ln\left(\frac{t}{{\psi'_D}}\right)^{\frac{2}{\alpha_D}} L_k^{\mu_D-1}(t) \Upsilon(\mu_E+i, \frac{{\psi'_E}t^{\frac{\alpha_E}{\alpha_D}}}{{\psi'_D}^{\frac{2}{\alpha_D}}})$. Similarly, I_2 can be solved utilizing [8, Eqs. (8.970.1) and (3.381.3)] to get

$$I_2 = \frac{4{\psi'_D}^{-\mu_D}}{\alpha_D \alpha_E {\psi'_E}^{\frac{2}{\alpha_E}}} \sum_{i=0}^{k} \frac{(-1)^i}{i!} \binom{k+\mu_D-1}{k-i} \sum_{j=1}^{N} w_j f_2(t_j), \quad (16)$$

where $f_2(t) = t^{\mu_E-1} \ln\left(\frac{t}{{\psi'_E}}\right)^{\frac{2}{\alpha_E}} L_k^{\mu_E-1}(t) \Gamma(\mu_D+i, \frac{{\psi'_D}t^{\frac{\alpha_D}{\alpha_E}}}{{\psi'_E}^{\frac{2}{\alpha_E}}})$. On substituting (15) and (16) into (14), the asymptotic ASC is obtained.

Remark 2: The asymptotic ASC depends on the correlation coefficient, ρ, but is independent of the average SNR, $\bar{\gamma}$.

B. Asymptotic SOP Analysis

For the asymptotic analysis, let us observe (12) and (13) at high values of $\bar{\gamma}_D$ for a constant $\bar{\gamma}_E$. It is noted that for high $\bar{\gamma}_D$, the dominant term in the expression for P_o corresponds to the smallest power of $\bar{\gamma}_D$. This occurs for $n = r = 0$. As a result, the asymptotic slope of the SOP curves is $\frac{\alpha_D\mu_D}{2}$, which indicates that the secrecy diversity order of the considered

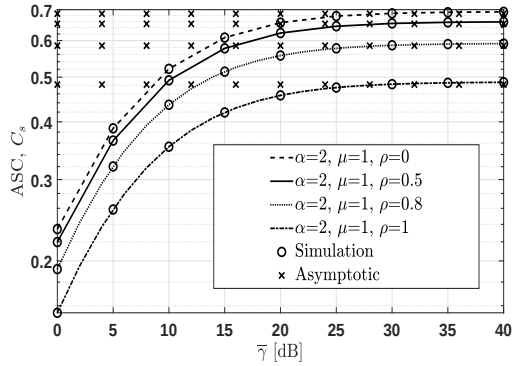

Fig. 1. Comparison of simulated, analytical (4), and asymptotic (14) ASC versus average SNR for different values of ρ.

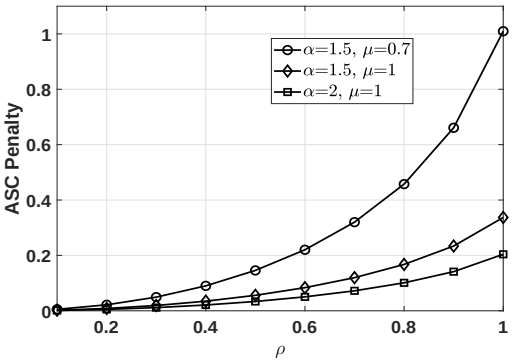

Fig. 2. Comparison of asymptotic ASC performance penalty versus ρ for different values of α and μ.

system depends only on the non-linearity and the multipath clusters of the main channel for a given $\bar{\gamma}_E$.

Remark 3: The asymptotic SOP performance will improve for a channel with less severe nonlinearity and more scattering clusters (i.e., greater values of α and μ). Using the asymptotic SOP analysis, it is possible to obtain the exact value of the correlation dependent horizontal shift or SNR penalty to achieve a given P_o which is elaborated in the description of Fig. 3.

VI. Numerical Results and Discussions

In this section, we plot the derived analytical results assuming that $\alpha_D = \alpha_E = \alpha$ and $\mu_D = \mu_E = \mu$. Although the derived exact expressions for ASC and SOP are expressed in terms of infinite series, these infinite summations converge quickly for finitely small values of k and r. To numerically evaluate the infinite series in (7), (8), (12), and (13), we have truncated the series in each expression to the same finite number of terms N = 10, which results in a sufficiently small truncation error. and the simulation results match with the analytical results upto fourth significant digit. The convergence of the infinite series can also be proved analytically using Cauchy Ratio test [19].

Fig. 1 shows a comparison of ASC for different values of ρ with $\alpha = 2$ and $\mu = 1$. It is seen from the figure that the ASC is better for lower ρ compared to the ASC for higher ρ. This is because a larger value of ρ represents a stronger correlation between the main and eavesdropper channels indicating that the eavesdropper is very close to the legitimate receiver. We also note from Fig. 1 that at high SNR, the ASC saturates and there is no further improvement in ASC, which is also corroborated by the asymptotic ASC analysis presented in Section V-A.

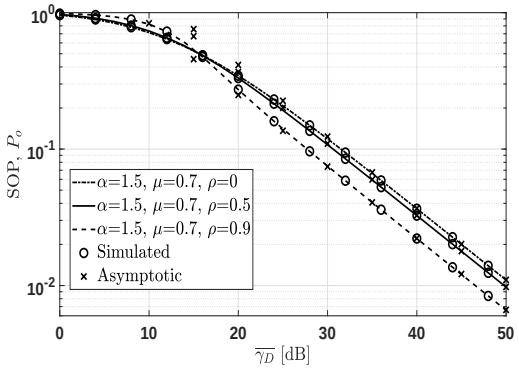

Fig. 3. Comparison of simulated, analytical (12), and asymptotic SOP versus $\bar{\gamma}_D$ for different values of ρ and $\bar{\gamma}_E$=10 dB.

The asymptotic ASC performance penalty due to correlation shown in 2 can be quantified by computing the difference between the asymptotic ASC using (14) and the asymptotic ASC using [7, Eq. (7)] for the uncorrelated main and eavesdropper channels. As seen from the figure, the ASC performance penalty increases with ρ. Moreover, the ASC performance penalty is lesser for higher values of α and μ which indicate better channel conditions.

A comparison of SOP for different values of ρ as a function of $\bar{\gamma}_D$ for $\bar{\gamma}_E$=10 dB with fixed R_s=1 is shown in Fig. 3. It is observed that as the value of ρ increases, the SOP performance improves for moderate to high $\bar{\gamma}_D$ while the converse is true for lower values of $\bar{\gamma}_D$. This observation is in line with the results obtained in [20]. Further, we observe that for ρ=0.5, the SOP is 0.03273 and 0.00977 at 40 dB and 50 dB SNR, respectively. Thus, the slope of the curve is $\log_{10}(0.03273) - \log_{10}(0.00977) = 0.525051 \approx 0.525 = \alpha_D\mu_D/2$, which is also justified by the asymptotic SOP analysis in Section V-B. Fig. 3 also highlights that the effect of correlation is to introduce some sort of horizontal shift or SNR penalty for a given SOP. For instance, for $P_o = 10^{-2}$, the required $\bar{\gamma}_D \approx 46$ dB for $\rho = 1$ while $\bar{\gamma}_D \approx 50$ dB for $\rho = 0.5$. This indicates an SNR penalty of around 4 dB. Moreover, this SNR penalty significantly depends on the correlation between the two channels because the penalty is low as ρ increases from 0.1 to 0.5 and and is higher when ρ increases from 0.5 to 1.

References

[1] Y. Wu *et al.*, "A survey of physical layer security techniques for 5G wireless networks and challenges ahead," *IEEE J. Sel. Areas Commun.*, vol. 36, no. 4, pp. 679–695, Apr. 2018.

[2] D.-S. Shiu *et al.*, "Fading correlation and its effect on the capacity of multielement antenna systems," *IEEE Trans. Commun.*, vol. 48, no. 3, pp. 502–513, Mar. 2000.

[3] H. Jeon *et al.*, "Bounds on secrecy capacity over correlated ergodic fading channels at high SNR," *IEEE Trans. Inf. Theory*, vol. 57, no. 4, pp. 1975–1983, Apr. 2011.

[4] G. Pan *et al.*, "Physical-layer security over non-small-scale fading channels," *IEEE Trans. Veh. Technol.*, vol. 65, no. 3, pp. 1326–1339, Mar. 2016.

[5] M. D. Yacoub, "The α-μ distribution: A physical fading model for the Stacy distribution," *IEEE Trans. Veh. Technol.*, vol. 56, no. 1, pp. 27–34, Jan. 2007.

[6] L. Kong *et al.*, "Performance analysis of physical layer security over α-μ fading channel," *Electron. Lett.*, vol. 52, no. 1, pp. 45–47, Jan. 2015.

[7] H. Lei *et al.*, "Secrecy capacity analysis over α-μ fading channels," *IEEE Commun. Lett.*, vol. 21, no. 6, pp. 1445–1448, Jun. 2017.

[8] I. S. Gradshteyn and I.M. Rhyzhik, *Table of Integrals, Series and Products*, 7th ed., A. Jeffrey and D. Zwillinger, Eds. Burlington, MA, USA: Academic Press, 2007.

[9] M. Abramowitz and I. A. Stegun, *Handbook of Mathematical Functions With Formulas, Graphs, and Mathematical Tables*, 9th ed. New York, NY, USA: Dover, 1972.

[10] A. D. Wyner, "The wire-tap channel," *Bell Syst. Tech. J.*, vol. 54, no. 8, pp. 1355–1387, Oct. 1975.
[11] R. A. A. de Souza and M. D. Yacoub, "On the mulitvariate α-μ distribution with arbitrary correlation and fading parameters," in *Proc. IEEE Intl. Conf. Commun. (ICC)*, Beijing, China, May 2008, pp. 4456–4460.
[12] A. Mathur *et al.*, "On physical layer security of α-η-κ-μ fading channels," *IEEE Commun. Lett.*, vol. 22, no. 10, pp. 2168–2171, Oct. 2018.
[13] Y. Ai *et al.*, "On physical layer security of double Rayleigh fading channels for vehicular communications," *IEEE Wireless Commun. Lett.*, 2018.
[14] A. P. Prudnikov *et al.*, *Integrals and Series*, vol. 3, New York: Gordon and Breach Science, 1990.
[15] M. D. Springer, *The Algebra of Random Variables*, New York, NY, USA: Wiley, 1979.
[16] P. K. Mittal and K. C. Gupta, "An integral involving generalized function of two variables," *Proc. Indian Acad. Sci.-Sec. A*, vol. 75, no. 3, pp. 117–123, Mar. 1972.
[17] K. Peppas, "A new formula for the average bit error probability of dual-hop amplify-and-forward relaying systems over generalized shadowed fading channels," *IEEE Wireless Commun. Lett.*, vol. 1, no. 2, pp. 85–88, Apr. 2012.
[18] V. S. Adamchik and O. I. Marichev, "The algorithm for calculating integrals of hypergeometric type functions and its realization in REDUCE system," in *Proc. Int. Conf. Symbolic and Algebraic Comput.*, pp. 212–224, Aug. 1990.
[19] G. Arfken, *Mathematical Methods for Physicists*, 3rd ed. Orlando, FL: Academic, 1985.
[20] N. S. Ferdinand *et al*, "Physical layer secrecy performance of TAS wiretap channels with correlated main and eavesdropper channels," *IEEE Wireless Commun. Lett.*, vol. 3, no. 1, pp. 86–89, Feb. 2014.